ARTICLE

How Graphene Oxide Quenches Fluorescence of Rhodamine 6G

Kai-li Fan[a], Zhen-kun Guo[a], Zhi-gang Geng[b], Jing Ge[a], Shen-long Jiang[b], Jia-hua Hu[a], Qun Zhang[a,b*]

a. Department of Chemical Physics, University of Science and Technology of China, Hefei 230026, China

b. Hefei National Laboratory for Physical Sciences at the Microscale, University of Science and Technology of China, Hefei 230026, China

(Dated: Received on March 18, 2013; Accepted on March 28, 2013)

We investigate the fluorescence quenching of Rhodamine 6G (R6G), a well known laser dye with a high fluorescence quantum yield, by as-synthesized graphene oxide (GO) in aqueous solution, which is found to be rather efficient. By means of steady-state and time-resolved fluorescence spectroscopy combined with detailed analysis about the linear absorption variation for this R6G-GO system, the pertinent quenching mechanism has been elucidated to be a combination of dynamic and static quenching. Possible ground-state complexes between R6G and GO during the static quenching have also been suggested. Furthermore, the direction of photoinduced electron transfer between R6G and GO has been discussed.

Key words: Graphene oxide, Rhodamine 6G, Fluorescence quenching, Interaction, Mechanism

I. INTRODUCTION

In order for graphene, the well-known "wonder material" [1, 2], to be truly effective in device applications in the post-silicon era, routes to its large-scale production must be developed. Graphene oxide (GO), readily derived from the exfoliation of graphite oxide, provides such an inexpensive route [3, 4] and has aroused tremendous interest over the past few years. Noticeably, this heightened interest is currently experiencing a shift from GO as a mere precursor of graphene to GO itself [4, 5], primarily owing to its heterogeneous chemical/electronic structures [6] and its potentials in a wide spectrum of applications [5, 7, 8]. For example, GO-based fluorescence quenching has recently been demonstrated to provide an ideal sensing platform for quantitative DNA analysis [9].

Fluorescence quenching is a subject that has received long-standing attention, which is, to a large extent, because it can serve as a valuable source of information about biochemical systems [10]. Although there have emerged a number of recent studies on fluorescence quenching of organic dyes by graphene [11−15], similar reports linked to GO [14, 16, 17] remain sparse. Obviously, in terms of biochemical applications, it would be favorable to replace graphene with GO as the latter bears excellent solution-processing compatibility. We also notice that the pertinent quenching mechanisms for both graphene and GO have seldom been addressed [15], and hence the research in this regard is desirable.

The present work is dedicated to gaining insight into the mechanism responsible for fluorescence quenching of Rhodamine 6G (R6G), a well known fluorescent probe, by as-synthesized GO in aqueous solution. Detailed examination on the steady-state and time-resolved fluorescence spectra of the R6G-GO system reveals that GO can effectively quench the fluorescence of R6G in a fashion of combined dynamic and static quenching. With the aid of linear absorption measurements, the insight into the possible ground-state complexes formed between R6G and GO during the course of static quenching is gained. Analysis from the electrochemistry perspective suggests that in terms of the photoinduced electron transfer quenching, the excited state of R6G molecule acts as an electron donor while GO as an electron acceptor.

II. EXPERIMENTS

The GO samples were as-synthesized using a modified Hummers method [18−20]. $K_2S_2O_8$ (2 g) and P_2O_5 (2 g) were added into 98%H_2SO_4 (10 mL), with the temperature increasing to 90 °C; graphite powder (2.4 g) was added into the mixture, and the solution was maintained at 80 °C for 4.5 h. The resultant preoxidized product was cleaned using deionized (DI) water and dried in air. After it was mixed with 98%H_2SO_4 (92 mL) and a slowly added $KMnO_4$ (12 g) at a temperature below 20 °C, DI water (180 mL) was added. After 2 h, additional DI water (560 mL) and 30%H_2O_2

*Author to whom correspondence should be addressed. E-mail: qunzh@ustc.edu.cn

(10 mL) were slowly added into the solution to completely react with the excess $KMnO_4$. The resultant bright-yellow solution was further washed several times with diluted HCl aqueous solution (1/10, volume ratio) and DI water. The brown-black powders of GO were obtained after drying the washed solution in a vacuum oven at −51 °C. Finally, 50 mg GO powders were dispersed into 50 mL DI water after a 10-min sonication, yielding the bright-yellow GO/water suspension (1.0 mg/mL) that was used as the stock solution. The concentration of the stock aqueous solutions of R6G was 64.6 μmol/L. For all the mixed R6G/GO solutions used in the experiments, the R6G concentration, [R6G], was kept constant at 32.3 μmol/L while that of GO, [GO], was varied from 0 to 200 μg/mL. Before each measurement the premixed solution was sonicated for 30 min to reach equilibrium.

High-purity graphite powder was purchased from Alfa Aesar. All the chemicals (H_2SO_4, P_2O_5, HCl, $KMnO_4$, and H_2O_2, Sinopharm Chemical Reagent Co., Ltd.; R6G, Exciton) are of analytical grade and were used as received without further purification. The deionized water was produced with a Millpore Milli-Q grade (resistivity ca. 18.5 MΩ/cm).

The linear absorption spectra were recorded on a SolidSpec-3700DUV UV-VIS-NIR spectrophotometer (Shimadzu). Raman measurements were conducted on a LABRAM-HR Raman spectrometer with an excitation wavelength of 514.5 nm provided by an Ar^+ laser. The C1s XPS spectra were obtained using an ESCALAB 250 (Thermo-VG Scientific). The steady-state and time-resolved fluorescence measurements were performed on an FLS920 fluorescence spectrometer (Edinburgh). All the steady-state fluorescence spectra (510−710 nm) were corrected against the sensitivity of the photomultiplier tube. For the fluorescence lifetime measurements, excitation at 470 nm was provided by an SC400-2 supercontinuum laser source (Fianium) with a 6-ps pulse width, and emission was monitored at 560 nm by means of time-correlated single photon counting. Fluorescence lifetimes were obtained by a least-squares fit of the experimental data with the instrument response function deconvoluted. All the measurements were carried out at the ambient conditions.

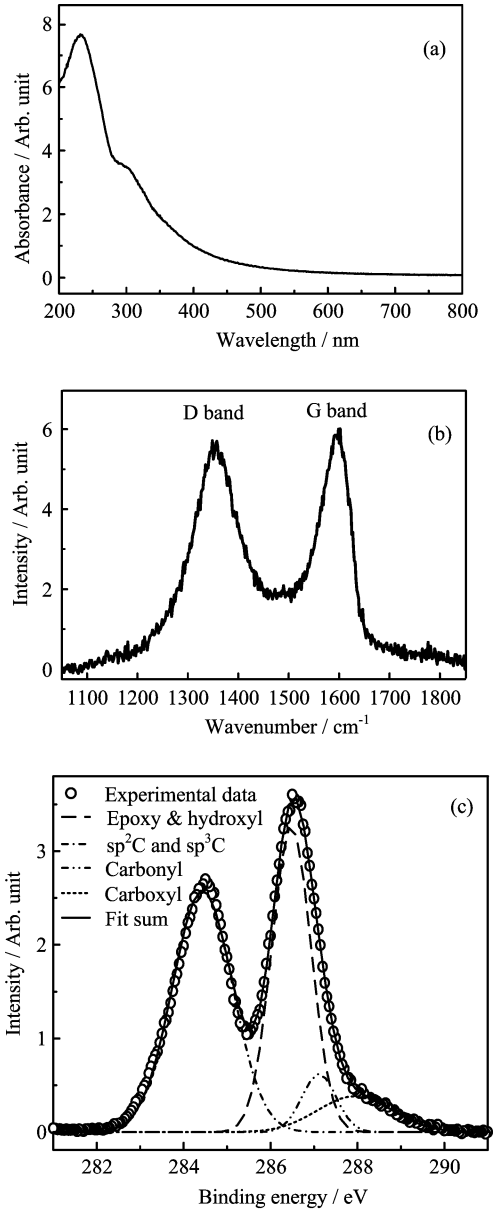

FIG. 1 Characterization of the as-synthesized GO sample. (a) Linear absorption spectrum, (b) Raman spectrum, and (c) C1s XPS spectrum.

III. RESULTS AND DISCUSSION

Figure 1(a) shows the linear absorption spectrum (200−800 nm) of as-synthesized GO, in which the two spectral features at ca. 230 and 300 nm correspond to the $\pi \rightarrow \pi^*$ transitions of aromatic C−C bonds and the $n \rightarrow \pi^*$ transitions of C=O bonds, respectively [21, 22]. GO has very weak absorption in the visible spectral region due to the destruction of conjugated π system. The Raman spectrum of as-synthesized GO, as shown in Fig.1(b), exhibits the well-resolved D and G bands [23, 24]. The D-band peaking at ca. 1350 cm^{-1} arises from the breathing modes in C−C ring structures, whose presence is indicative of a disordered graphitic carbon lattice, and hence the defects in GO. The G band peaking at ca. 1600 cm^{-1} emerges as a result of the $C(sp^2)-C(sp^2)$ bond stretching vibrations. Figure 1(c) displays the C1s X-ray photoelectron spectroscopy (XPS) spectrum of as-synthesized GO, which can be well deconvolved into four bands, peaking at 284.4, 286.5, 287.1, and 288.0 eV, respectively. The 284.4-eV band originates from carbon atoms forming C−C/C=C bonds, while the other three bands are associated with various oxidation groups, as annotated within the plot. The spectral assignments are in ac-

DOI:10.1063/1674-0068/26/03/252-258

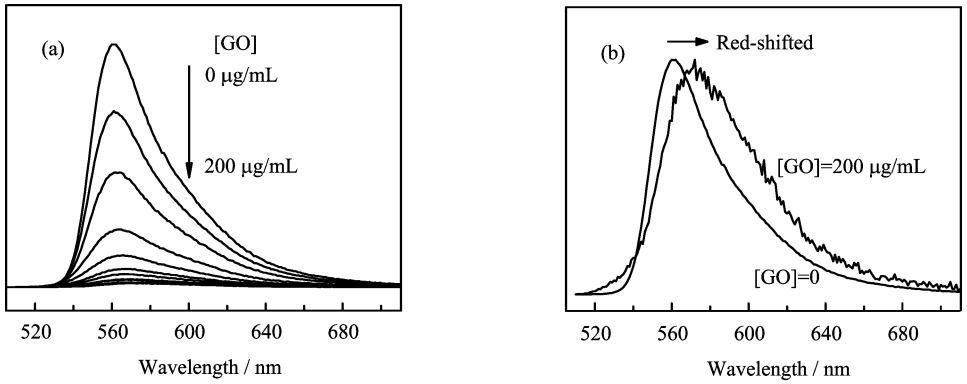

FIG. 2 (a) Steady-state fluorescence spectra of the R6G-GO system recorded with [R6G] fixed at 32.3 μmol/L and [GO]=0, 10, 20, 40, 60, 80, 100, 125, 150, 175, and 200 μg/mL. (b) Intensity-normalized emission at [GO]=200 μg/mL is red-shifted by ca. 8 nm with respect to that at [GO]=0 μg/mL.

cordance with the previous reports [25−27]. From the relative areas for these bands, the atomic C/O ratio can be readily determined to be ca. 2.7/1, a typical value that agrees well with the documented values for as-synthesized GO [26, 27].

As shown in Fig.2(a), the fluorescence emission intensity of R6G gradually decreases with [GO], increasing. As [GO] reaches 200 μg/mL, the fluorescence nearly vanishes. This indicates that GO is indeed an efficient quencher of the R6G fluorescence. In addition, an obvious red-shift of ca. 8 nm occurs in the intensity-normalized emission as [GO] changes from 0 to 200 μg/mL (Fig.2(b)).

Fluorescence quenching can be generally categorized into static and dynamic regimes. In terms of dynamic (or collisional) quenching, it follows the well-known Stern-Volmer equation (normally under steady-state approximation and with continuous excitation) [10],

$$\frac{F_0}{F} = \frac{\tau_0}{\tau} = 1 + k_q\tau_0[\mathrm{Q}] = 1 + K_\mathrm{D}[\mathrm{Q}] \tag{1}$$

where $F_0(F)$ is the fluorescence intensity in the absence (presence) of quencher, k_q is the bimolecular quenching constant, $\tau_0(\tau)$ is the lifetime of the fluorophores in the absence (presence) of quencher, and [Q] is the concentration of quencher. Plotting F_0/F as a function of [Q] is expected to yield the linear slope $K_\mathrm{D}(=k_q\tau_0)$, a characteristic constant for dynamic quenching. On the other hand, static quenching featuring the formation of the ground-state complex between the fluorophore and the quencher is described by [10],

$$\frac{F_0}{F} = 1 + K_\mathrm{S}[\mathrm{Q}] \tag{2}$$

Although the relationship of F_0/F versus $[Q]$ is still linear herein, the aforementioned K_D is replaced with the association constant K_S.

In the R6G-GO system under examination, the dependence of F_0/F on [Q] evidently deviates from linearity, as can be clearly seen in Fig.3(a). This indicates

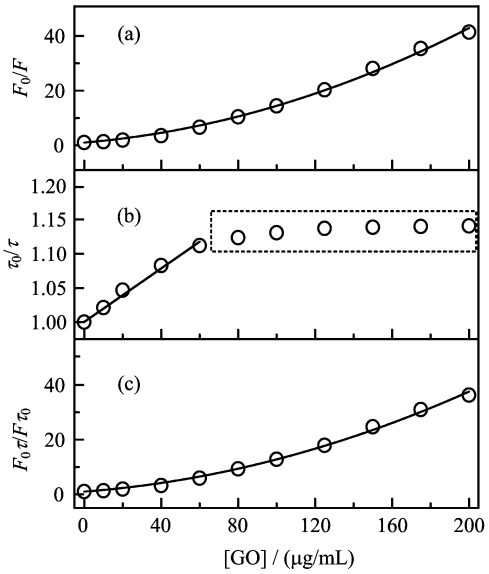

FIG. 3 Fluorescence quenching of R6G by GO: (a) F_0/F *vs.* [GO], (b) τ_0/τ *vs.* [GO], (c) $(F_0\tau)/(F\tau_0)$ *vs.* [GO]. $F_0(F)$ is the R6G fluorescence intensity in the absence (presence) of GO and τ_0 (τ) is the fluorescence lifetime of R6G in the absence (presence) of GO. Curve fitting (solid lines) is performed with a fixed intercept at 1.

that the quenching of R6G fluorescence by GO cannot solely be described by either dynamic or static mechanism. For such kind of nonlinear quenching behavior, the classical quenching sphere action model [10, 28] is often adopted [29]. Under this model, the Stern-Volmer equation reads

$$\frac{F_0}{F} = (1 + K_\mathrm{D}[Q])\exp([Q]VN_\mathrm{A}) \tag{3}$$

where V is the volume of the sphere and N_A is the Avogadro constant. For our as-synthesized GO samples existing in a form of flake, the average lateral size is ca. 45 μm, which means that a single GO flake contains ca.

DOI:10.1063/1674-0068/26/03/252-258

7.8×10^{10} carbon atoms. Taking into account the atomic C/O ratio of ca. 2.7/1 from the XPS analysis, the molar weight of a single GO flake can be estimated to be ca. 1.4×10^{12} g/mol. As such, [GO] in mass concentrations ranging from 0 to 200 μg/mL translates to molar concentrations in the range of $0-1.4\times10^{-16}$ mol/cm^3. Since the effective remote quenching distance of GO is ca. 30 nm [11, 12] which can be approximated as the radius of the sphere under the quenching sphere action model, the $[Q]VN_A$ term under our experimental conditions roughly falls within the range of $0-9.3\times10^{-9}$. Therefore, the exponential term in Eq.(3) is nearly unity for all [GO], making Eq.(3) reduce to Eq.(1). Apparently, the quenching sphere action model is not suited to describe the nonlinear quenching behavior, as shown in Fig.3(a).

Intuitively, the quenching mechanism responsible for our R6G-GO system most likely falls in a regime that combines the dynamic and static quenching, which could be analyzed in a separate manner [15]. As dynamic quenching results from the collisions of the excited fluorophores with the quenchers, a preferable way to distinguish between dynamic and static quenching is to perform lifetime measurements. In Fig.3(b), we plot τ_0/τ versus [GO], the relevant data are given in Table I. τ_0/τ linearly increases as [GO] increases from 0 to 60 μg/mL, yielding $K_D=9.8\times10^{-4}$ (μg/mL)$^{-1}$ (or equivalently, $k_q=2.2\times10^5$ (μg/mL)$^{-1}$s^{-1}) according to Eq.(1). This indicates that dynamic quenching dominates in the lower [GO] region (≤60 μg/mL). When [GO] exceeds 60 μg/mL, obvious deviation from linear dependence of τ_0/τ on [GO] is observed, manifesting itself as a plateau (dashed box in Fig.3(b)). The appearance of such a plateau can be understood as follows. Abundantly, small R6G molecules are sandwiched in between the much larger GO flakes. The inter-flake distance decreases as [GO] increases, but should reach sort of equilibrium due to the electrostatic repulsion between adjacent GO flakes that are negatively charged due to the hydroxyl and carboxyl groups decorating the graphene planes and edges [4, 30]. In light of our observation of the critical changeover (from linear rise to plateau) occurring at 60 μg/mL (Fig.3(b)), such an equilibrium distance can be estimated to be ca. 13 μm (based on the effective carbon-atom area that is ca. 2.6 Å^2 when the C−C bond length, 1.42 Å, in GO [31] is considered). The mean-free path of the photoexcited R6G* molecules that randomly move between the GO flakes gradually decreases as [GO] increases until the equilibrium distance is reached. This makes the lifetime τ of the R6G* molecules decrease before [GO] is increased to the critical concentration of 60 μg/mL and afterwards remains nearly unaltered. The lifetime saturation effect observed in the R6G-GO system, which is definitely not attributed to the dynamic quenching, should point to the static quenching that features the formation of the ground-state R6G-GO complex.

For such kind of combined dynamic and static quenching that manifests itself as an upward curvature [10] (Fig.3(a)), the total quenching efficiency as a collective result of both quenching can normally be decomposed according to [10, 15]

$$\frac{F_0}{F} = (1+K_D[Q])(1+K_S[Q]) = \frac{\tau_0}{\tau}(1+K_S[Q]) \quad (4)$$

or equivalently,

$$\frac{F_0\tau}{F\tau_0} = 1+K_S[Q] \quad (5)$$

However, plotting $(F_0\tau)/(F\tau_0)$ versus [GO] (Fig.3(c)) does not produce the expected linear dependence as described by Eq.(5). Instead, the curve fit turns out to be of a quadratic form

$$\frac{F_0\tau}{F\tau_0} = 1+C_1[Q]+C_2[Q]^2 \quad (6)$$

where $C_1=(2.67\pm0.47)\times10^{-2}$ (μg/mL)$^{-1}$ and $C_2=(1.58\pm0.14)\times10^{-4}$ (μg/mL)$^{-2}$. From this observation, we can safely infer that the static quenching in the R6G-GO system involves more than one ground-state complex, which cannot be described by a mere association constant K_S as in Eq.(5).

To gain further insight into the possible ground-state complexes between R6G and GO during the course of static quenching, we have also recorded the absorption spectra for all the mixed R6G/GO solutions used in the fluorescence measurements. Figure 4(a) exhibits several representative absorption spectra (all subtracted with respect to the GO absorption background). The main peak at ca. 525 nm initially drops as [GO] increases until 60 μg/mL (indicated by a downward arrow in Fig.4) and afterwards slightly goes up (indicated

TABLE I The fluorescence lifetimes of R6G as a function of [GO] ranging from 0 to 200 μg/mL. All the lifetime fit quality parameters χ^2 are close to unity, which means that all the fits are good. The fluorescence is excited at 470 nm and monitored at 560 nm.

[GO]/(μg/mL)	τ/ns	χ^2	τ_0/τ
0	4.48[a]	1.10	1.000
10	4.39	1.06	1.021
20	4.28	1.08	1.047
40	4.13	1.07	1.085
60	4.03	1.00	1.112
80	3.97	1.02	1.128
100	3.95	0.99	1.134
125	3.94	1.00	1.137
150	3.93	1.04	1.140
175	3.93	1.04	1.140
200	3.93	1.03	1.140

[a] τ_0=4.48 ns.

DOI:10.1063/1674-0068/26/03/252-258

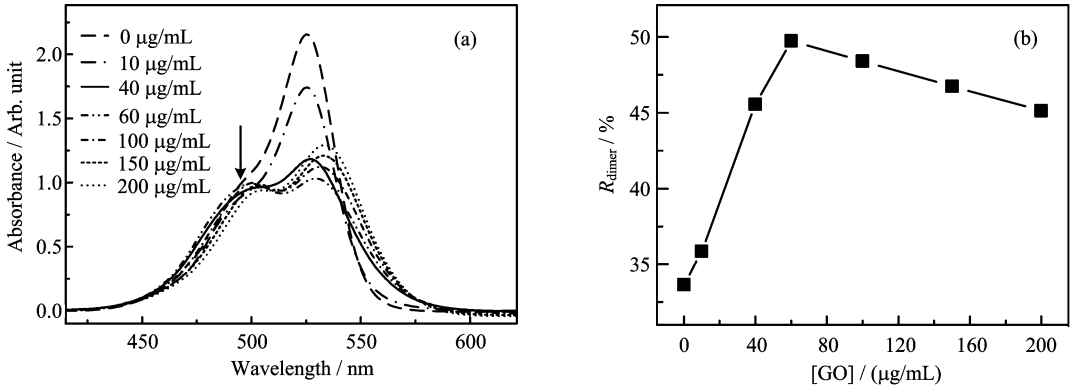

FIG. 4 (a) Representative linear absorption spectra recorded at different [GO]. These spectra are all subtracted with respect to the GO absorption background. (b) [GO]-dependent absorbance ratios ($R_{\rm dimer}$) of the dimer peak (indicted by a downward arrow in (a)).

by an upward arrow in Fig.4). This intensity variation is accompanied by spectral red-shift as well as broadening. As [GO] varies from 0 to 200 μg/mL, the total red-shift amounts to ca. 9 nm, a value that is nearly identical to that observed in the fluorescence spectra (Fig.2(b)). The red-shift is indicative of the formation of the ground-state R6G-GO complex, while the broadening is a reflection of the strong ionic and π-π stacking between R6G and GO [32]. To a certain extent, GO, with its weakly ionizable carboxylic groups, can be viewed as a low-strength acid resin, allowing ion exchange interactions with charged molecules to form molecular complexes [5].

Interestingly, it can be seen from Fig.4 that the shoulder at ca. 500 nm (indicted by a downward arrow in Fig.1(a)), a signature of the dimerization of R6G monomers [13, 33], becomes more pronounced with [GO] increasing. As [GO]≥60 μg/mL there occurs an iso-absorptive wavelength at ca. 510 nm, which is located at the junction of the 500 nm dimer peak and the 525 nm main peak. This implies the coexistence of the R6G dimerization and the R6G-GO complex formation. Figure 4(b) shows the absorbance ratios ($R_{\rm dimer}$) of the dimer peak (defined as the dimer-peak absorbance divided by the absorbance sum of the dimer and main peaks) at different [GO], from which one can see that the critical changeover occurs again at [GO]=60 μg/mL. On one hand, collision-induced dimerization dominates in the lower [GO] region ([GO]≤60 μg/mL); the explanation for the drastic increase of $R_{\rm dimer}$ with [GO] increasing is in line with that for the dynamic quenching discussed above. On the other hand, when [GO] is larger than 60 μg/mL, a slow drop of $R_{\rm dimer}$ appears with [GO] increasing. Such a slow drop (instead of a plateau in Fig.3(b)) can be understood in terms of the fact that, with [GO] increasing in the higher [GO] region ([GO]≥60 μg/mL), the number of the active sites (onto which the R6G monomers or dimers are bound) increases, making the tendency for the formation of the R6G-GO complexes prevails over the R6G dimerization. In addition, unlike the 525-nm main peaks, the 500-nm dimer peaks at different [GO] do not possess the corresponding mirror-image features in the fluorescence spectra (Fig.2(a)), which indicates that the R6G dimers are of the nonfluorescent H-type [34].

Considering that Eq.(6) responsible for static quenching may contain useful information about the R6G-GO complex formation, we here rewrite Eq.(6) of a quadratic form as

$$\frac{F_0\tau}{F\tau_0} = (1 + K_{\rm S}^{(1)}[{\rm Q}])(1 + K_{\rm S}^{(2)}[{\rm Q}]) \tag{7}$$

where $K_{\rm S}^{(1)}$=8.86×10^{-3} (μg/mL)$^{-1}$, and $K_{\rm S}^{(2)}$= 1.78×10^{-2} (μg/mL)$^{-1}$. Interestingly, $K_{\rm S}^{(2)}\approx 2K_{\rm S}^{(1)}$, based on which it is probable that two equilibrium processes co-exist:

$$\mathrm{R6G} + \mathrm{GO} \xleftrightarrow{K_{\rm S}^{(1)}} \mathrm{R6G}\cdot\mathrm{GO} \tag{8}$$

$$(\mathrm{R6G})_2 + \mathrm{GO} \xleftrightarrow{K_{\rm S}^{(2)}} (\mathrm{R6G})_2\cdot\mathrm{GO} \tag{9}$$

In our R6G-GO system, the number of the R6G molecules is much larger than that of the GO flakes, thus it is reasonable to assume that [R6G·GO]≈[(R6G)$_2$·GO]. This could lead to $K_{\rm S}^{(2)}\approx 2K_{\rm S}^{(1)}$ when [(R6G)$_2$]=[R6G]/2 is taken into account.

Furthermore, it is worth noting that there is essentially no overlap between the absorption spectrum of GO (Fig.1(a)) and the steady-state fluorescence emission band carried by the photoexcited R6G* molecules (Fig.2(a)). Basically, this suggests that electron transfer (instead of resonant energy transfer) between R6G* and GO may take effect herein [13, 14]. Then, how about the direction of such an electron transfer process, either from R6G* to GO or from GO to R6G*? To answer this, one needs to evaluate the work functions of R6G* and GO from a perspective of electrochemistry.

DOI:10.1063/1674-0068/26/03/252-258

R6G is known to have an oxidation potential of 1.22 V and a reduction potential of −0.6 V (versus normal hydrogen electrode, NHE) [35]. The singlet-state energy of R6G is ca. 2.28 eV, which is estimated by half the energy sum of the absorption and fluorescence maxima (similar treatment can be found [36]). Thus, the oxidation and reduction potentials of R6G* are ca. −1.06 and 1.68 V, respectively, and the redox potential (versus NHE) of R6G* equals ca. −2.74 V. Since the average value of the NHE potential (with respect to the vacuum level), −4.5 eV, is usually adopted [37, 38], the work function of R6G* can be estimated to be ca. −1.76 eV. Considering that the work function of GO can be regarded as the energy of conduction band (ca. −3.50 eV [39]), one can readily reach a conclusion that the electron transfer from R6G* to GO is thermodynamically favorable. It is well accepted that among others (such as intersystem crossing or the heavy atom effect and electron exchange or Dexter interactions), photoinduced electron transfer (PET) is one of the major mechanisms responsible for fluorescence quenching [10]. In terms of PET, a complex is formed between the electron donor and the electron acceptor. The more common situation is when the excited state of a fluorophore acts as an electron acceptor, whereas PET quenching can also occur by electron transfer from the excited fluorophore to the quencher [40−43], as observed in our R6G-GO system.

IV. CONCLUSION

In summary, it is found that the fluorescence of R6G can be effectively quenched by as-synthesized GO in aqueous solution. By examining the steady-state and time-resolved fluorescence combined with linear absorption measurements, we reveal that a combined dynamic and static quenching accounts for such an efficient quenching. Possible ground-state complexes as well as the direction of photoinduced electron transfer in this R6G-GO system have been discussed.

V. ACKNOWLEDGMENTS

This work was supported by the National Basic Research Program of China (No.2010CB923300), the National Natural Science Foundation of China (No.91127042 and No.21173205), the Chinese Academy of Sciences (No.XDB01020000), the FRFCUC (No.WK2340000012), the USTC-NSRL Joint Funds (No.KY2340000021), and the National Undergraduate Innovative Training Program of Ministry of Education (No.201210358064).

[1] A. K. Geim and K. S. Novoselov, Nature Mater. **6**, 183 (2007).
[2] A. K. Geim, Science **324**, 1530 (2009).
[3] S. Park and R. S. Ruoff, Nature Nanotechnol. **4**, 217 (2009).
[4] D. A. Dikin, S. Stankovich, E. J. Zimney, R. D. Piner, G. H. B. Dommett, G. Evmenenko, S. T. Nguyen, and R. S. Ruoff, Nature (London) **448**, 457 (2007).
[5] K. P. Loh, Q. L. Bao, G. Eda, and M. Chhowalla, Nature Chem. **2**, 1015 (2010).
[6] D. R. Dreyer, S. Park, C. W. Bielawski, and R. S. Ruoff, Chem. Soc. Rev. **39**, 228 (2010).
[7] S. Stankovich, D. A. Dikin, G. H. B. Dommett, K. M. Kohlhaas, E. J. Zimney, E. A. Stach, R. D. Piner, S. T. Nguyen, and R. S. Ruoff, Nature (London) **442**, 282 (2006).
[8] G. Eda and M. Chhowalla, Adv. Mater. **22**, 2392 (2010).
[9] S. He, B. Song, D. Li, C. Zhu, W. Qi, Y. Wen, L. Wang, S. Song, H. Fang, and C. Fan, Adv. Funct. Mater. **20**, 453 (2010).
[10] J. R. Lakowicz, *Principles of Fluorescence Spectroscopy*, New York: Springer, (2006).
[11] R. S. Swathi and K. L. Sebastian, J. Chem. Phys. **129**, 054703 (2008).
[12] R. S. Swathi and K. L. Sebastian, J. Chem. Phys. **130**, 086101 (2009).
[13] Y. Pang, Y. Cui, Y. Ma, H. Qian, and X. Shen, Micro Nano Lett. **7**, 608 (2012).
[14] Y. Liu, C. Liu, and Y. Liu, Appl. Surf. Sci. **257**, 5513 (2011).
[15] X. Zhang and F. Li, J. Photochem. Photobio. A **246**, 8 (2012).
[16] E. Treossi, M. Melucci, A. Liscio, M. Gazzano, P. Samorì, and V. Palermo, J. Am. Chem. Soc. **131**, 15576 (2009).
[17] J. Balapanuru, J. Yang, S. Xiao, Q. Bao, M. Jahan, L. Polavarapu, J. Wei, Q. Xu, and K. P. Loh, Angew. Chem. Int. Ed. **49**, 6549 (2010).
[18] W. S. Hummers and R. E. Offeman, J. Am. Chem. Soc. **80**, 1339 (1958).
[19] D. V. Kosynkin, A. L. Higginbotham, A. Sinitskii, J. R. Lomeda, A. Dimiev, B. K. Price, and J. M. Tour, Nature (London) **458**, 872 (2009).
[20] D. C. Marcano, D. V. Kosynkin, J. M. Berlin, A. Sinitskii, Z. Sun, A. Slesarev, L. B. Alemany, W. Lu, and J. M. Tour, ACS Nano **4**, 4806 (2010).
[21] R. Li, X. Liu, X. Deng, S. Zhang, Q. He, and X. Chang, Mater. Lett. **76**, 247 (2012).
[22] J. I. Paredes, S. V. Rodil, A. M. Alonso, and J. M. D. Tascón, Langmuir **24**, 10560 (2008).
[23] S. Stankovich, D. A. Dikin, R. D. Piner, K. A. Kohlhaas, A. Kleinhammes, Y. Jia, Y. Wu, S. T. Nguyen, and R. S. Ruoff, Carbon **45**, 1558 (2007).
[24] K. N. Kudin, B. Ozbas, H. C. Schniepp, R. K. Prud'homme, I. A. Aksay, and R. Car, Nano Lett. **8**, 36 (2008).
[25] J. Zhang, H. Yang, G. Shen, P. Cheng, J. Zhang, and S. Guo, Chem. Commun. 1112 (2010).
[26] Z. J. Fan, W. Kai, J. Yan, T. Wei, L. J. Zhi, J. Feng, Y. M. Ren, L. P. Song, and F. Wei, ACS Nano **5**, 191

(2011).
[27] X. Mei and J. Ouyang, Carbon 49, 5389 (2011).
[28] I. M. Frank and S. I. Vavilov, Z Phys. **69**, 100 (1931).
[29] H. Zeng and G. Durocher, J. Lumin. **63**, 75 (1995).
[30] K. P. Loh, Q. Bao, P. K. Ang, and J. Yang, J. Mater. Chem. **20**, 2277 (2010).
[31] J. Zhou, Q. Wang, Q. Sun, X. S. Chen, Y. Kawazoe, and P. Jena, Nano Lett. **9**, 3867 (2009).
[32] X. Wang, Y. He, and G. Song, Phys. Procedia **25**, 394 (2012).
[33] P. Ilich, P. K. Mishra, S. Macura, and T. P. Burghardt, Spectrochim. Acta A **52**, 1323 (1996).
[34] V. M. Martínez, F. L. Arbeloa, J. B. Prieto, and I. L. Arbeloa, J. Phys. Chem. B **109**, 7443 (2005).
[35] C. A. M. Seidel, J. Phys. Chem. **100**, 5541 (1996).
[36] M. Julliard and M. Chanon, Chem. Rev. **83**, 425 (1983).
[37] R. Memming, Top. Curr. Chem. **169**, 105 (1994).
[38] M. Sadeghi, W. Liu, T. G. Zhang, P. Stavropoulos, and B. Levy, J. Phys. Chem. **100**, 19466 (1996).
[39] T. F. Yeh, J. M. Syu, C. Cheng, T. H. Chang, and H. Teng, Adv. Funct. Mater. **20**, 2255 (2010).
[40] R. Vos and Y. Engelborghs, Photochem. Photobio. **60**, 24 (1994).
[41] M. Suzuki, M. Sano, M. Kimura, K. Hanabusa, and H. Shirai, Eur. Polym. J. **35**, 221 (1999).
[42] K. Nagai, J. Tsukamoto, N. Takamiya, and M. Kancko, J. Phys. Chem. **99**, 6648 (1995).
[43] A. H. A. Clayton, K. P. Ghiggino, G. J. Wilson, P. J. Keyte, and M. N. Paddon-Row, Chem. Phys. Lett. **195**, 249 (1992).

DOI:10.1063/1674-0068/26/03/252-258